Rearrangement of Azirine Intermediates to Nitriles: Theoretical Study of Cleavage of 3,4-Dihydro-1a*H*-Azirine[2,3-*c*]Pyrrol-2-One to Cyanoketene–Formaldimine Complex

SATURNINO CALVO-LOSADA,[1] JOSÉ JOAQUÍN QUIRANTE,[1] DIMAS SUÁREZ,[2] TOMÁS LUIS SORDO[2]

[1]*Departamento de Química Física, Universidad de Málaga, Campus de Teatinos, 29071 Málaga, Spain*
[2]*Departamento de Química Física y Analítica, Universidad de Oviedo, Julián Clavería, 33006 Oviedo, Spain*

Received 3 November 1997; accepted 16 January 1998

ABSTRACT: A detailed investigation of the reaction path for the thermal rearrangement of 3,4-dihydro-1a*H*-azirine[2,3-*c*]pyrrol-2-one to yield a cyanoketene–formaldimine complex is carried out at the MP2/6-31G* and B3LYP/6-31G* levels of theory. The ring opening of the five-membered pyrrolinone ring and the formation of the nitrile group takes place in a concerted manner, presenting a significant strain energy release and allowing for an electronic stabilization by coarctate conjugation of the transition structure (TS). These two factors make possible a moderate energy barrier. Although the structural features B3LYP/6-31G* theoretical levels, it is found that the MP2 energy barrier (28.8 CCSD(T)/6-31G*//MP2/6-31G* value (17.1 kcal/mol). The complex electronic rearrangement can be rationalized using the theory of coarctate transition structures developed by Herges as the evolution of an azirine structure without referring to a hypothetical vinyl nitrene intermediate.
 J Comput Chem 19: 912–922, 1998

Keywords: bicyclic azirine intermediates; ring cleavage; *ab initio* calculations; DFT calculations; coarctate transition structures

Correspondence to: T. L. Sordo
Contract/grant sponsor: DGICYT; contract grant number: PB94-1314-C03-01

 CCC 0192-8651 / 98 / 080912-11

Introduction

The pyrolitic fragmentation[1,2] of appropriately substituted vinyl azides to nitriles has been investigated extensively by Moore and coworkers,[3,4] establishing that cyclic vinyl azides thermally cleave to zwitterionic intermediates in a process referred to as a zwittazido cleavage reaction. Particularly interesting is the ring contraction of the 4-azido-2-pyrrolinones to the 3-cyano-2-azetidinones passing through the zwitterionic intermediates, which have also been found in the [2 + 2] cycloaddition reaction of ketenes with imines known as the Staudinger reaction.[5–8]

We have recently carried out an extensive theoretical study[8] of the zwittazido cleavage reaction of the 4-azido-2-pyrrolinones in which different mechanisms[9] for thermolysis have been investigated. The kinetic controlling step corresponds to the loss of a N_2 molecule leading to an azirine intermediate that rearranges in a concerted process to a more stable cyanoketene–formaldimine complex (see Scheme 1). From the mechanistic point of view, cleavage of the pyrrolinone ring is of great interest because a notable electronic reorganization is implied.

Assuming vinyl nitrenes as intermediates, it has been shown that an extended Hückel–Möbius model is useful to rationalize consistently the decomposition of vinyl azides as a class of concerted processes termed complex reactions.[10] The linear succession of bond making and breaking is completed by *terminators* at both ends connected through a linear subsystem. According to this generalized model, a cyclic array of p atomic orbitals describing a pericyclic transition structure (TS) can be topologically transformed, without loss of its Hückel–Möbius character, into a homeomorphic array in which one center has two orthogonal p atomic orbitals. The resultant set of p atomic orbitals describes a *coarctate* TS for a complex reaction that is stabilized by conjugation similar to the pericyclic reactions. However, in the aforementioned theoretical study[8] no vinyl nitrene structure has been located on the corresponding PES. Therefore, it is necessary to examine this coarctate model to verify and quantify its qualitative statements for the ring opening of 3,4-dihydro-1a*H*-azirine[2,3-*c*]pyrrol-2-one with the aid of quantum chemical calculations at various levels of theory.

Methods

Quantum chemical calculations were carried out with the Gaussian-94 system of programs.[11] Stable species were fully optimized and TS located by means of the Schlegel algorithm[12] at the HF/6-31G* and MP2(FC)/6-31G* levels of theory.[13] All critical points were further characterized and the ZPVE was evaluated by analytical computations of harmonic frequencies at the MP2(FC)/6-31G* level. Thermodynamic gas-phase data (298.15 K, 1 bar) were computed to obtain results more readily comparable with experiment within the ideal gas, rigid rotor, and harmonic oscillator approximations.[14] In addition, MP4SDTQ/6-31G*, QCISD(T)/6-31G*, and CCSD(T)/6-31G* single-point calculations were carried out on the MP2/6-31G* geometries to estimate the effect of higher levels of theory on the calculated relative energies.

Density functional calculations[15] were carried out by means of the hybrid functional developed by Becke (usually denoted B3LYP[16,17]) to assess its performance as compared with conventional *ab*

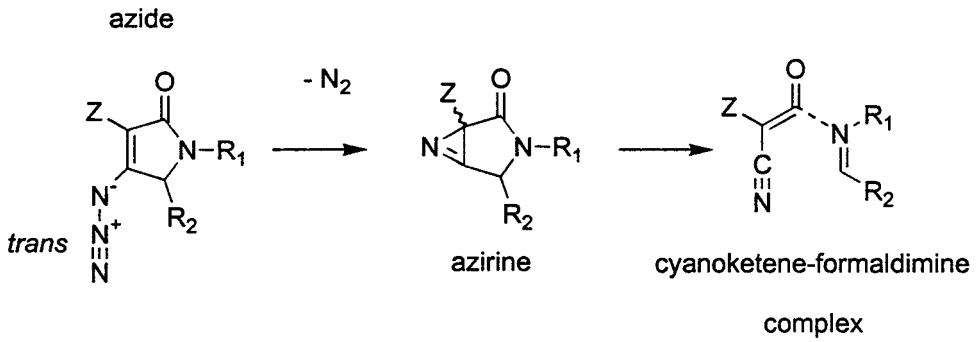

SCHEME 1.

initio methodologies. All the structures reported were further optimized at the B3LYP/6-31G* level and characterized by the corresponding frequency calculations. The influence of larger basis sets on the relative energies of the MP2/6-31G*- and B3LYP/6-31G*-optimized structures was estimated by means of single-point calculations using the 6-311 + G(3df,2p) basis set.[13] Reaction paths passing through the TS studied in this work were followed by MP2/6-31G* and B3LYP/6-31G* intrinsic reaction coordinate (IRC)[18] calculations using the González and Schlegel algorithm.[19]

Following the theory of atoms in molecules developed by Bader,[20] we carried out a topological analysis of the bond critical points (BCP) of the electronic density, $\rho(\vec{r})$, for the most significant structures in this work. The values of $\rho(\vec{r})$, $\nabla^2\rho(\vec{r})$, and of the local energy density $H(\vec{r})$ at the BCPs permit characterization of the interatomic interactions.[20] The ellipticity, ε, of the charge density at the BCPs is defined as $\varepsilon = \lambda_1/\lambda_2 - 1$, where λ_1 and λ_2 are the eigenvalues of the Hessian matrix of $\rho(\vec{r})$ corresponding to the eigenvectors perpendicular to the bond path. This magnitude provides a measure of the π accumulation of the charge density for multiple bonds. The BCP analysis employed a recent version of the EXTREME program, a part of the AIMPAC suite of programs,[21] and the MORPHY program developed by Popelier.[22] Atomic charges were computed using natural population analysis[23] on the corresponding density matrices.

Results

2*H*-AZIRINE

To estimate the effect of the fused five-membered pyrrolinone ring on the three-membered azirine heterocycle in 3,4-dihydro-1a*H*-azirine[2,3-*c*]pyrrol-2-one, 2*H*-azirine was investigated using various levels of theory. Table I shows the calculated equilibrium geometries and the strain energies computed from the corresponding homodesmic process.[24] All theory levels coincide in predicting a C2—N bond distance very close to a typical C—N double bond (about 1.26 Å), whereas the C3—N bond distance (1.55 Å) is 0.1 Å greater than ordinary C—N single bonds. The calculated strain energies amount to 44.6 and 46.7 kcal/mol at the MP2/6-31G* and B3LYP/6-31G* levels, respectively. According to our calculations, the corresponding values for the isoelectronic cyclopropene ring are about 10 kcal/mol higher than for 2*H*-azirine at the same levels of theory. The MP2/6-31G* and B3LYP/6-31G* analytical calculation of the force constants gives frequency values of 702 and 723 cm^{-1}, respectively, for the N—C2—C3 bending mode (or, alternatively, the N—C3 stretching mode).

The topological analysis of the electronic density of 2*H*-azirine at the B3LYP/6-31G* and QCISD/6-31G* levels render a (3, +1) critical point that characterizes the appearance of a three-

TABLE I.
Optimized Structure and Homodesmic Strain Energy[a] (kcal / mol) of 2*H*-Azirine Computed Using Various Levels of Theory (Distances in Angstroms and Angles in Degrees).

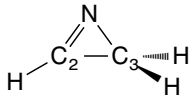

2*H*-azirine

Level	C_2—N	C_3—N	C_2—C_3	N—C_3—C_2	C_3—C_2—N	ΔE_H^a
MP2 / 6-31G*	1.273	1.564	1.445	49.9	69.9	−44.6
B3LYP / 6-31G*	1.256	1.550	1.450	49.4	69.5	−46.7
QCISD / 6-31G*	1.264	1.551	1.451	49.7	69.3	—
MP2 / 6-311 + G(3df,2p)	1.263	1.553	1.446	50.0	69.9	—
B3LYP / 6-311 + G(3df,2p)	1.246	1.545	1.447	49.1	69.5	—

[a]The strain energy of 2*H*-azirine is estimated by computing the reaction energy of the following homodesmic reaction:

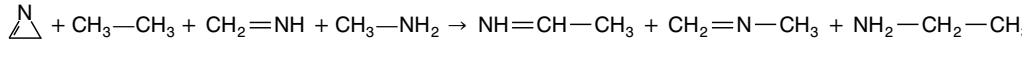

membered ring.[25] The corresponding (3, −1) BCPs were also located and present similar properties at both levels of theory. In agreement with geometrical data, the C3—N BCP has lower values of ρ (0.22 a.u.), and $\nabla^2\rho$ (−0.134 and −0.155 a.u. at B3LYP/6-31G* and QCISD/6-31G* levels, respectively) than those values normally obtained for a typical single C—N bond ($\rho = 0.271$ a.u. and $\nabla^2\rho = -0.802$ a.u. for *N*-methylformaldimine at the B3LYP/6-31G* level). The ellipticity, ε, of the C3—N bond is extremely large (3.480 and 2.748 at B3LYP/6-31G* and QCISD/6-31G* levels, respectively) indicating an asymmetric distribution of the charge density around the corresponding bond path. All these structural and electronic data allow us to conclude that the C3—N single bond at 2*H*-azirine corresponds to a moderate bonding interaction intermediate between typical shared and closed-shell interactions.[20]

AZIRINE INTERMEDIATE

Figure 1 displays the optimized structure of the azirine intermediate (3,4-dihydro-1a*H*-azirine[2,3-*c*]pyrrol-2-one) at the MP2/6-31G* and B3LYP/6-31G* levels. It is clear from this figure that no significant differences between MP2 and B3LYP geometries can be observed. The most remarkable characteristic of this compound is the notable distortion of the five-membered heterocycle (see, e.g., C4—C5—N and C2—C3—C4 angles) as a consequence of the fused three-membered ring of the azirine ring. The azirine ring is not placed coplanar with the pyrrolinone ring (C2—C3—C4—N7: 111.8° and 115.0° at the MP2/6-31G* and B3LYP/6-31G* levels, respectively; see Fig. 1). Thus, the equilibrium geometry of 3,4-dihydro-1a*H*-azirine[2,3-*c*]pyrrol-2-one corresponds to a strained structure in which the C3 and C4 atoms show a distorted tetrahedral and trigonal character, respectively. Conversely, the three-membered ring of the azirine group does not exhibit a distorted structure compared with that of 2*H*-azirine.

A complete analysis of the charge density of the azirine intermediate renders nearly coincident features of the BCP properties at the B3LYP/6-31G* and MP2/6-31G* levels and, therefore, Table II provides the B3LYP/6-31G* results. In contrast with the previously discussed 2*H*-azirine structure, in the case of the azirine intermediate, no BCP between the C3 and N7 atoms and no (3, +1) critical point associated with the C3—C4—N7

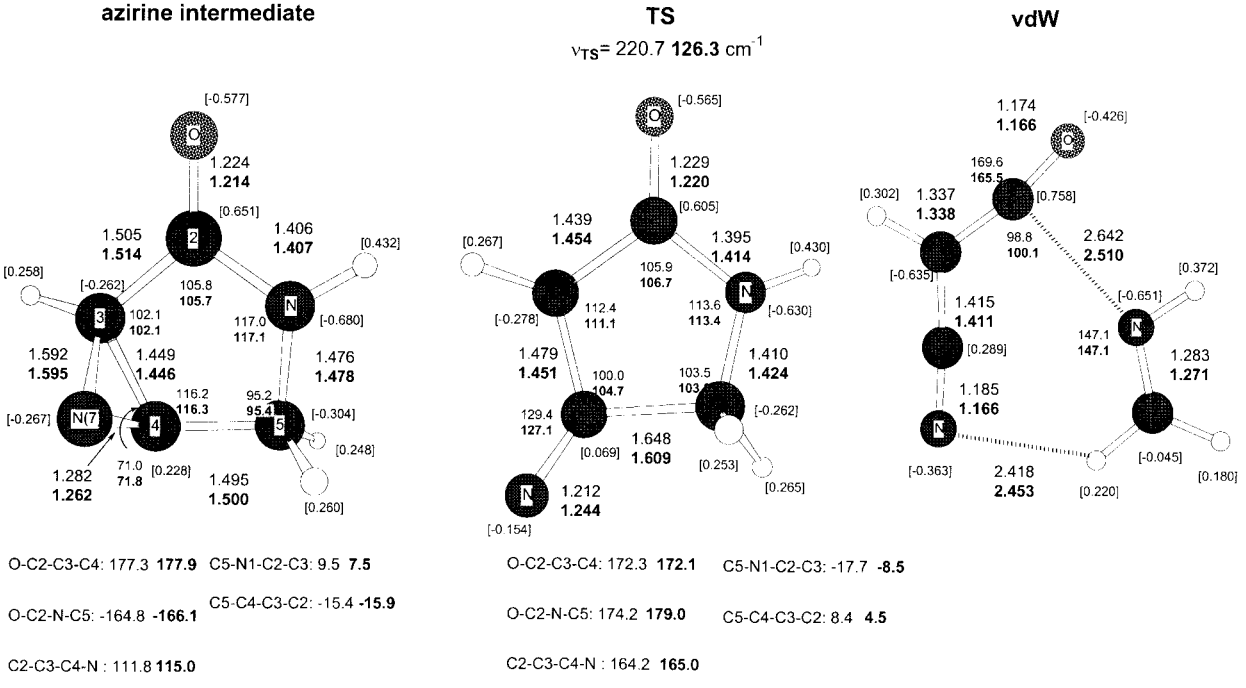

FIGURE 1. MP2 / 6-31G* and B3LYP / 6-31G* (in boldface) optimized structures. Distances in angstroms and angles in degrees. B3LYP / 6-31G* natural atomic charges are shown in brackets.

atoms were located. Nevertheless, the properties of the charge density evaluated in an appropriately selected point between C3 and N7 atoms are comparable to those corresponding to the weak C3—N bond of 2*H*-azirine (see Table II).[26] Then, the small elongation of the C3—N7 single bond (about 0.04 Å) in the azirine intermediate compared with 2*H*-azirine is reflected in a change of the topology of the charge density. On the other hand, the high ellipticity values of the N1—C2, C2—O6, C2—C3, and C3—C4 BCPs, together with the quasiplanarity of that part of the molecule (see the O—C2—C3—C4 dihedral angle in Fig. 1), can be interpreted in terms of a certain degree of electronic delocalization throughout these bonds. Finally, the C4—C5 bond presents the lowest charge and local energy densities[27] (see Table II) reflecting the susceptibility of this bond to be thermally cleft.

TRANSITION STRUCTURE

The TS for the ring opening of 3,4-dihydro-1a*H*-azirine[2,3-*c*]pyrrol-2-one to yield a cyanoketene plus formaldimine complex is shown in Figure 1. We can see that the three-membered ring of the azirine is entirely lost at the TS, while the C4—N7 bond distance decreases at 0.07 Å (MP2/6-31G*) or 0.02 Å (B3LYP/6-31G*). The evolution of the bond distances and bond angles of the pyrrolinone ring results in a less strained structure at the TS (the C4—C5—N1 angle increases to 103° degrees and the C3 and C4 atoms adopt a nearly trigonal character compared with the reactant) and starts to cleave through the elongation of the C4—C5 bond. This elongation is more accentuated by the MP2 method, which in general renders a later structure for this TS (C4—C5 bond length is 1.648 Å at the MP2/6-31G* level and 1.609 Å at B3LYP/6-31G*; see also C5—N1 bond and C5—N1—C2—C3 dihedral angle in Fig. 1). Both MP2/6-31G* and B3LYP/6-31G* levels of theory show a very similar transition vector, as shown in Scheme 2. The main components of this transition vector are the C3—C4—N7 bending motion, the CH_2 ring puckering, and a simultaneous rotation of the C5—N1 bond. These last motions play an important role in avoiding the small-angle strain in the ring opening of pyrrolinone.

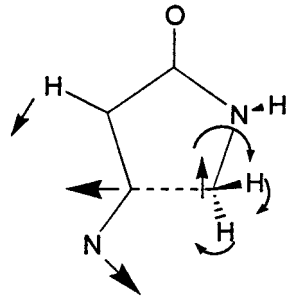

SCHEME 2.

TABLE II.
Bond Critical Point Properties[a] (a.u.) of Azirine Intermediate at B3LYP / 6-31G* Level of Theory.

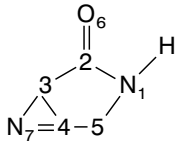

	$\rho(r_c)$	$\nabla^2\rho(r_c)$	ε	λ_1	λ_2	λ_3	r_1	r_2	$H(r_c)$
C5—N1	0.257	−0.678	0.058	−0.511	−0.483	0.316	1.140	1.652	−0.276
N1—C2	0.297	−0.921	0.120	−0.630	−0.563	0.272	1.660	0.999	−0.411
C2—C3	0.260	−0.620	0.118	−0.525	−0.470	0.375	1.453	1.410	−0.218
C3—C4	0.270	−0.561	0.304	−0.519	−0.398	0.355	1.338	1.409	−0.248
C4—C5	0.251	−0.585	0.012	−0.470	−0.465	0.350	1.462	1.376	−0.210
C2—O6	0.411	0.101	0.104	−1.091	−0.987	2.180	0.762	1.533	−0.703
C4—N7	0.392	−0.593	0.121	−0.810	−0.723	0.940	0.816	1.576	−0.694
C3—N7[b]	0.210	−0.103	3.214	−0.364	−0.086	0.804	1.266	1.748	−0.158

[a] $\rho(r_c)$, $\nabla^2\rho(r_c)$, and ε stand for the electronic density, Laplacian of the electronic density, and ellipticity at BCP, respectively, λ_1, λ_2, and λ_3 represent the corresponding eigenvalues of the Hessian of the charge density at BCP. r_1 and r_2 are the distances from the critical point to A and B on the bond A—B. $H(r_c)$ is the local energy density: $H(r_c) = G(r_c) + V(r_c)$ (see refs. 10 and 27).
[b] These properties of the charge density were computed on an appropriate point between C4 and N7 nuclei because the corresponding critical point was not located.

TABLE III.
Bond Critical Point Properties[a] (au) of the TS for the Ring-Opening of Azirine Intermediate at the B3LYP / 6-31G* Theory Level

	$\rho(r_c)$	$\nabla^2\rho(r_c)$	ε	λ_1	λ_2	λ_3	r_1	r_2	$H(r_c)$
C_5—N_1	0.286	−0.880	0.067	−0.579	−0.542	0.240	1.022	1.669	−0.380
N_1—C_2	0.293	−0.905	0.122	−0.628	−0.559	0.281	1.654	1.018	−0.394
C_2—C_3	0.284	−0.725	0.204	−0.598	−0.497	0.370	1.382	1.367	−0.261
C_3—C_4	0.282	−0.685	0.150	−0.564	−0.481	0.350	1.323	1.385	−0.263
C_4—C_5	0.202	−0.363	0.052	−0.361	−0.343	0.341	1.534	1.505	−0.142
C_2—O_6	0.407	0.018	0.094	−1.067	−0.975	2.060	0.766	1.539	−0.697
C_4—N_7	0.415	−0.568	0.108	−0.956	−0.862	1.250	0.794	1.556	−0.739

[a] $\rho(r_c)$, $\nabla^2\rho(r_c)$ and ε stands for the electronic density, Laplacian of the electronic density and ellipticity at BCP, respectively. λ_1, λ_2 and λ_3 represent the corresponding eigenvalues of the Hessian of the charge density at BCP. r_1 and r_2 are the distances from the critical point to A and B in the bond A—B. $H(r_c)$ is the local energy density: $H(r_c) = G(r_c) + V(r_c)$ (see refs. 10 and 27).

The rearrangement of the electronic density at the TS is also conveniently discussed in terms of the corresponding BCP properties. Table III shows the BCP properties for the TS at the B3LYP/6-31G* level of theory. When comparing these properties with those corresponding to the azirine intermediate (see Table II), we see that the breaking C4—C5 bond presents an important reduction (0.05 a.u.) of the charge density at the corresponding BCP, whereas the amount of charge density at the BCPs for the adjacent bonds remains unchanged or increases slightly. The shortening of the C4—N7 bond distance and the increase of charge density at its BCP indicate that the nitrile group is partially formed at this TS. This is clearly confirmed by the computed C4—N7 bond orders[28] at the MP2/6-31G* level (1.97, 2.78, and 2.90 for reactant, TS, and product, respectively) and at B3LYP/6-31G* level (2.02, 2.28, and 2.99). On the other hand, the magnitude of the eigenvalues associated with the perpendicular eigenvectors to the bond path for the C4—C3, C3—C2, C2—N1, and C5—N1 bonds becomes more important at the TS than at the reactant. This fact allows one to interpret the electronic rearrangement throughout the TS skeleton as a preferential π accumulation of charge density.

The energy barrier for the ring opening of the azirine intermediate was computed using various levels of theory (see Table IV). The HF/6-31G* MP2/6-31G* levels give energy barriers of 16.5 and 29.8 kcal/mol, respectively, whereas the more elaborate N-electron treatments by the MP4SDTQ/6-31G*, QCISD(T)/6-31G*, and CCSD(T)/6-31G* levels predict barriers of 22.3, 16.1, and 17.1 kcal/mol, respectively. Thus, a substantial improvement of the correlated method tends to reduce the MP2/6-31G* activation energy by more than 10 kcal/mol. The B3LYP correlation-exchange energy functional predicts a certain decrease in the energy barrier with respect to the *ab initio* results, given that, at the B3LYP/6-31G* level, only 12.4 kcal/mol are required to cleave the azirine intermediate. Therefore, despite

TABLE IV.
Relative Energies (kcal / mol) of Structures Considered in This Work Optimized at MP2 / 6-31G* and B3LYP / 6-31G* Levels of Theory.

Structures	HF / 6-31G*[a,b]	MP2 / 6-31G*[a]	MP4 6-31G*[c]	QCISD(T) / 6-31G*[c]	CCSD(T) / 6-31G*[b]	MP2 / 6-311 + G(3df,2p)[c]	B3LYP / 6-31G*[a]	B3LYP / 6-311 + G(3df,2p)[d]
Azirine intermediate	0.0 (0.0)	0.0 (0.0)	0.0	0.0	0.0	0.0	0.0 (0.0)	0.0
TS	16.5 (−1.0)	29.8 (−1.5)	22.3	16.1	17.1	28.8	12.4 (−1.4)	11.6
Cyanoketene–formaldimine vdW cis-complex	−29.1 (−2.9)	−19.2 (−3.8)	−22.7	−19.8	−19.5	−16.5	−18.8 (−3.3)	−23.5

[a] ZPVE correction in parentheses.
[b] HF results are included to appreciate the correlation contributions.
[c] Single-point calculations on the MP2 / 6-31G* geometries.
[d] Single-point calculations on the B3LYP / 6-31G* geometries.

the structural and electronic similarities between the B3LYP/6-31G* and MP2/6-31G* TSs, we note that, interestingly, the B3LYP/6-31G* activation energy is much closer to the CCSD(T) or QCISD(T) values than to the MP2/6-31G* value. On the other hand, augmentation of the basis set shows a moderate effect given that the MP2/6-31G* and B3LYP/6-31G* energy barriers are reduced by about 1.0 kcal/mol at the MP2/6-311 + G(3df,2p)//MP2/6-31G* and B3LYP/6-311 + G(3df,2p)//B3LYP/6-31G* levels (see Table IV). The calculated enthalpy and free energy of activation[29] amount to 13.9 and 14.0 kcal/mol, respectively, at the highest *ab initio* level used,[29a] and 9.9 and 10.5 kcal/mol, respectively, using the DFT results.[29b]

REACTION PATH

The reaction path for the ring opening of the azirine intermediate was followed by means of IRC calculations at the MP2/6-31G* and B3LYP/6-31G* levels, with the observed geometrical evolution being very similar at both levels. Figure 2 displays the evolution of some bond distances involved in the reaction coordinate at the MP2/6-31G* level and the MP2/6-31G* and B3LYP/6-31G* energy profiles. The most important internal motion from the azirine intermediate to TS is the N7—C4—C3 bending (see C3—N7 bond distance in Fig. 2), concomitant with the ring puckering of the CH_2 group and the rehybridization of the C4 and C3 atoms. At the same time, a charge transfer of 0.10 and 0.05 e from the formaldimine moiety to the cyanoketene part of the molecule is observed at the B3LYP/6-31G* and MP2/6-31G* levels, respectively. A dramatic change of the components of the reaction coordinate is observed in Figure 2 after the TS. The distance of the breaking C4—C5 bond, and, to a lesser extent, the C2—N1 bond distance, dominate the reaction coordinate along the product channel on the PES. On the other hand, there are remarkable differences in the corresponding MP2 and

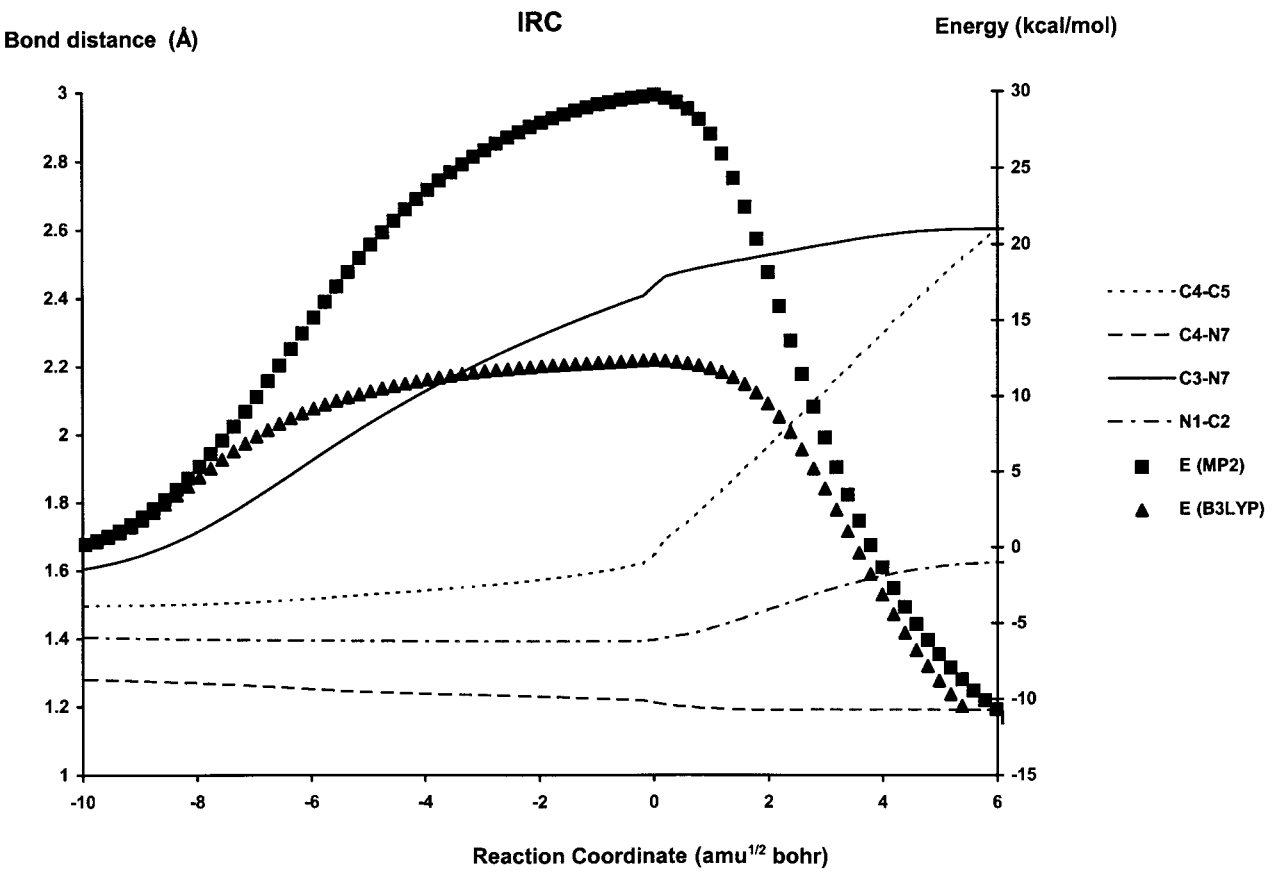

FIGURE 2. IRC energy profiles obtained at the MP2 / 6-31G* and B3LYP / 6-31G* levels. Geometrical evolution of the MP2 / 6-31G* IRC is also shown.

B3LYP energy profiles in Figure 2. In effect, as mentioned earlier, the predicted energy barriers are quite divergent: 12.4 kcal/mol (B3LYP/6-31G*) vs. 29.8 kcal/mol (MP2/6-31G*). Moreover, the curvature of the energy profile in the neighborhood of the TS is much smoother at B3LYP/6-31G* level than at MP2/6-31G*.

The role of the bending motion of the C3—C4—N7 atoms in the reaction coordinate may be of interest to assess the stability of azirine intermediates produced by pyrolysis of cyclic vinyl azides.[1,8] Considering the fragile nature of the C3—N7 bond and the low frequency of the C3—C4—N7 bending mode (585 cm^{-1} at the MP2/6-31G* level, 702 cm^{-1} for 2*H*-azirine) level, it seems reasonable to expect that some part of the energy release from the corresponding TS for the pyrolysis of vinyl azides may be channeled into the bending motion of the resultant azirine group thus facilitating a rapid decomposition of the 3,4-dihydro-1a*H*-azirine[2,3-*c*]pyrrol-2-one intermediates.

CYANOKETENE–FORMALDIMINE VAN DER WAALS COMPLEX

The subsequent evolution of the system after passing the TS leads to a planar van der Waals cis-complex between cyanoketene and formaldimine fragments (''vdW'' in Fig. 1). Previous theoretical studies[7,8] have shown that the stability of the ketene-imine intermediates is very dependent on the theoretical approach used, on the electrostatic effect of solvent, and on the electronic and steric effects of substituents. At the MP2/6-31G* level, this complex has a C(ketene)—N(imine) bond distance of 2.642 Å and the charge transfer from formaldimine to cyanoketene amounts to 0.038 e. The computed reaction energy at the HF/6-31G* and MP2/6-31G* levels is −29.1 and −19.2 kcal/mol, respectively, whereas the MP4/6-31G*, QCISD(T)/6-31G*, and CCSD(T)/6-31G* single-point calculations on the MP2/6-31G* geometries render values of −22.7, −19.8, and −19.5 kcal/mol, respectively. This vdW complex was also studied by using the B3LYP/6-31G* level, providing results close to the *ab initio* ones.[31] The B3LYP/6-31G* reaction energy is −18.8 kcal/mol whereas the corresponding C(ketene)—N(imine) bond distance and the charge transfer are 2.510 Å and 0.121 e, respectively. At the MP2/6-311 + G(3df,2p)//MP2/6-31G* and B3LYP/6-311 + G(3df,2p)//B3LYP/6-31G* levels the relative energy of the vdW complex amounts to −16.5 and −23.5 kcal/mol (see Table IV). Finally, the *ab initio*-calculated reaction enthalpy and free energy are −19.0 and −24.1 kcal/mol, respectively (−24.4 and −29.0 kcal/mol, according to DFT results).[29]

Discussion

All theoretical results on the different aspects of this reactive process (structure, electronic rearrangement, energetics, etc.) are useful for investigation of the quite complex cleavage of the azirine intermediate. In particular, analysis of the charge density and the geometrical features of the TS for the ring opening of 3,4-dihydro-1a*H*-azirine[2,3-*c*]pyrrol-2-one allow us to invoke a certain electronic delocalization involving the nitrile group and the rest of the atomic centers in the five-membered ring. Moreover, in the framework of the theory of coarctate transition states we propose that only six electrons released from the lone pair of N1, the distorted σ C4—C5 orbital, and one π orbital of the C4—N7 group may be considered to be specially *active* at this TS. These six active electrons can be devised to establish a Hückel conjugation along a *coarctate* array of p atomic orbitals as depicted in Scheme 3.

Figure 3 contains a computer plot of some of the highest occupied Kohn–Sham orbitals calculated at the B3LYP/6-31G* level on the geometry of the corresponding TS (MP2/6-31G* natural orbitals were also plotted presenting nearly an identical aspect). An examination of the localization and nodal properties of these orbitals demonstrates that the Hückel conjugation described in Scheme 3 is clearly present in the calculated electronic structure of the TS (especially interesting is the conjugation between the nitrile group and the C—C breaking bond represented by the HOMO-3 orbital; see Fig. 3). According to our calculations this Hückel electronic delocalization at the TS may be a

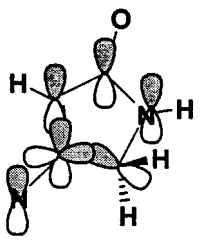

SCHEME 3.

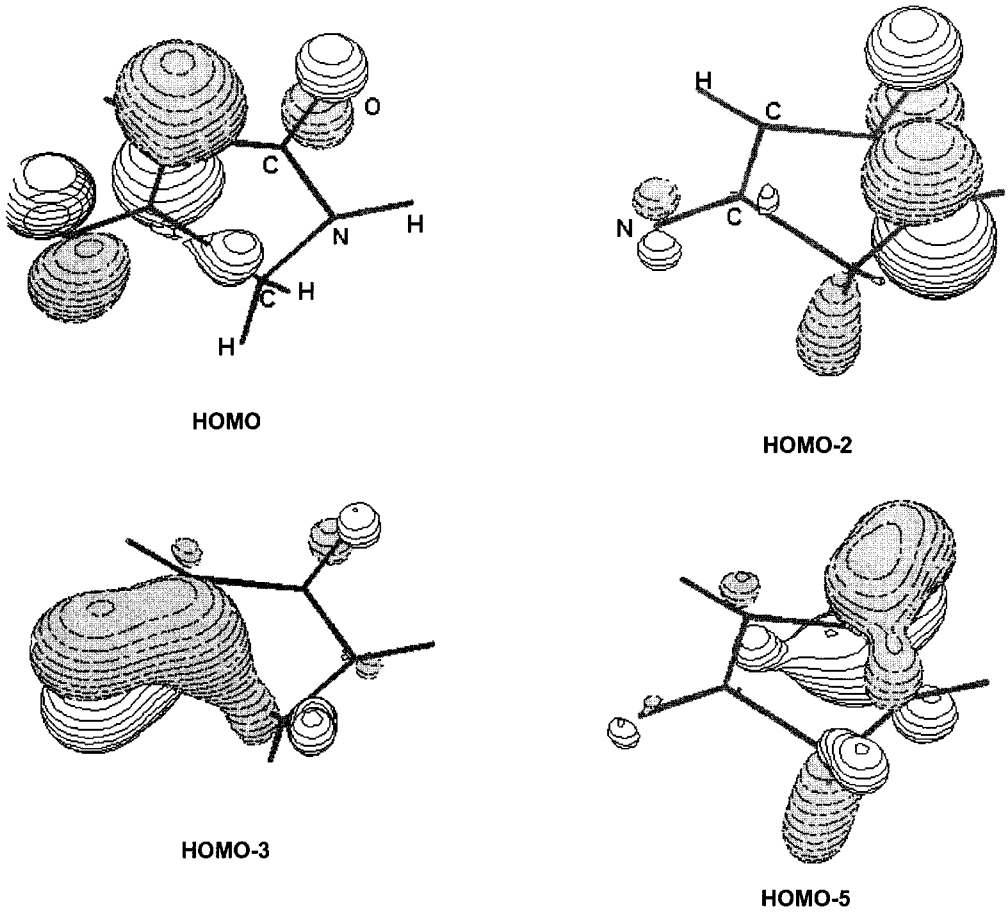

FIGURE 3. Computer plot of various Kohn–Sham MO of TS obtained at the B3LYP / 6-31G* level.

factor contributing to the moderate energy barrier presented by this process [17.1 and 12.4 kcal/mol at the CCSD(T)/6-31G*//MP2/6-31G* and B3LYP/6-31G* levels, respectively].

As previously mentioned, the thermolysis of 4-azido-2-pyrrolinone leads to the formation of an unstable azirine intermediate that presents a clearly formed C4—N7 double bond, a fragile C3—N7 single bond, and two strained fused rings. In addition, the reaction coordinate from the azirine intermediate to the TS is dominated by the N7—C4—C3 bending and the CH_2 ring puckering motions. Interestingly, these components of the reaction coordinate may be interpreted as the most efficient internal motions leading to the stabilization of the TS—thanks to the release of the strain energy of the rings and to the Hückel conjugation of the six active electrons.

The theory of coarctate TSs explains the thermal decomposition of cyclic vinyl azides passing through vinyl nitrene intermediates, which evolve through a subsequent coarctate TSs. However, no such nitrene intermediate has been located on the MP2/6-31G* and B3LYP/6-31G* PES for the thermolysis of 4-azido-2-pyrrolinone,[8] and our theoretical results clearly show that no vinyl nitrene intermediate is required to account for the feasibility of this particular *coarctate* process. In effect, instead of a lone pair and five-membered ring terminators linked by a linear subsystem structure for the TS,[10] we find that, in the azirine opening, the exocyclic π C—N bond acts simultaneously as both the electronic terminator and the linear subsystem required to establish the coarctate conjugation with the five-membered ring terminator.

Summary

A detailed analysis of the structure and charge density of 2*H*-azirine reveals that the C—N single bond in azirine intermediates has a small covalent character. According to our theoretical calculations, the thermal ring opening of 3,4-dihydro-

1a *H*-azirine[2,3-*c*]pyrrol-2-one is a concerted process. The analysis of the geometry and charge density shows that, at the TS, the nitrile group is partially formed and a certain π electronic delocalization, involving both the five-membered heterocycle and the exocyclic nitrile group, is established. CCSD(T)/6-31G*//MP2/6-31G* calculations predict that the energy barrier has a value of 17.1 kcal/mol. The B3LYP/6-31G* and MP2/6-31G* values are 12.4 and 29.8 kcal/mol, respectively, rendering the DFT method a much flatter PES in the neighborhood of the TS and an energy barrier closer to that of CCSD(T) than the MP2 method. Both MP2/6-31G* and B3LYP/6-31G levels render a cyanoketene–formaldimine van der Waals cis-complex as the reaction product in the gas phase. This complex is 19.5, 19.2, and 18.8 kcal/mol more stable than the azirine intermediate at the CCSD(T)/6-31G*//MP2/6-31G*, MP2/6-31G*, and B3LYP/6-31G* levels, respectively.

The reaction coordinate is dominated by the bending motion of the azirine group and the puckering of the pyrrolinone ring, thus allowing a certain release of strain energy from the azirine intermediate and the appearance of an allowed Hückel conjugation of six electrons throughout the coarctate TS. These two factors could contribute to the moderate magnitude of the calculated energy barrier. The entire electronic rearrangement can be rationalized using the model developed by Herges as the evolution of an azirine structure without referring to a hypothetical vinyl nitrene intermediate.

Acknowledgments

The authors thank to CICYT (Spain) for a generous allocation of computer time on the Cray J90 at the CIEMAT. S.C.L. and J.J.Q. are grateful to the CICA (Junta de Andalucía) for the use of computing facilities.

References

1. A. Hassner, In *Azides and Nitrenes*: *Reactivity and Utility*, E. F. V. Scriven, Ed., Academic Press, New York, 1984.
2. A. Hassner, N. H. Wiegand, and H. E. Gottlieb, *J. Org. Chem.*, **51,** 3176 (1986).
3. (a) H. W. Moore and D. M. Goldish, In *The Chemistry of Halides, Pseudo-Halides and Azides* (*Supplement D*), S. Patai and Z. Rappoport, Eds., John Wiley & Sons, New York, 1983; (b) H. W. Moore, *Acc. Chem. Res.*, **12,** 125 (1979).
4. (a) H. W. Moore, L. Hernández, D. M. Kuner, F. Mercer, and A. Sing, *J. Am. Chem. Soc.*, **103,** 1769 (1981); (b) an interesting isoelectronic system has also been studied recently by Sander et al.: W. Sander, R. Albers, P. Komminck, and H. Wandel Liebigs, *Ann. Chem.*, 901 (1997).
5. G. I. Georg and V. T. Ravikumar, In *The Organic Chemistry of β-Lactams*, G. I. Georg, Ed., VCH, New York, 1993.
6. (a) J. Pacansky, J. S. Chang, D. W. Brown, and W. Schwarz, *J. Org. Chem.*, **47,** 2233 (1981); (b) H. W. Moore, G. Hughes, K. Srinivasachar, M. Fernández, N. V. Nguyen, D. Schoon, and A. Trahne, *J. Org. Chem.*, **50,** 4231 (1985).
7. (a) J. A. Sordo, J. González, and T. L. Sordo, *J. Am. Chem. Soc.*, **114,** 6249 (1992); (b) R. López, T. L. Sordo, J. A. Sordo, and J. González, *J. Org. Chem.*, **58,** 3263 (1993); (c) R. López, D. Suárez, M. F. Ruiz-López, J. González, J. A. Sordo, and T. L. Sordo, *J. Chem. Soc. Chem. Commun.*, 1677 (1995); (d) R. López, M. F. Ruiz-López, D. Rinaldi, J. A. Sordo, and T. L. Sordo, *J. Phys. Chem.*, **100,** 10600 (1996); (e) F. P. Cossío, J. M. Ugalde, X. López, B. Lecea, and C. Palomo, *J. Am. Chem. Soc.*, **115,** 995 (1993); (f) F. P. Cossío, A. Arrieta, B. Lecea, and J. M. Ugalde, *J. Am. Chem. Soc.*, **116,** 2085 (1994); (g) B. Lecea, I. Arrastia, A. Arrieta, G. Roa, X. López, M. I. Arriortua, J. M. Ugalde, and F. P. Cossío, *J. Org. Chem.*, **61,** 3070 (1996).
8. D. Suárez and T. L. Sordo, *J. Am. Chem. Soc.*, **119,** 10291 (1997).
9. Previous theoretical work on the thermolysis of vynilazides: (a) L. A. Burke, G. Leroy, M. Nguyen, and M. Sana, *J. Am. Chem. Soc.*, **100,** 3668 (1978); (b) H. R. Bock, R. Dammel, and S. Aygen, *J. Am. Chem. Soc.*, **105,** 7681 (1983); (c) T. Yamabe, M. Kaminoyama, T. Mintao, K. Hori, K. Isomura, and H. Taniguchi, *Tetrahedron*, **40,** 2095 (1984); (d) L. I. Lohr, M. Hanamura, and K. Morokuma, *J. Am. Chem. Soc.*, **105,** 5541 (1983).
10. R. Herges, *Angew. Chem. Int. Ed. Engl.*, **33,** 255 (1994).
11. M. J. Frisch, G. W. Trucks, H. B. Schlegel, P. M. W. Gill, B. G. Johnson, M. A. Robb, J. R. Cheeseman, T. Keith, G. A. Petersson, J. A. Montgomery, K. Raghavachari, M. A. Al-Laham, V. G. Zakrzewski, J. V. Ortiz, J. B. Foresman, C. Y. Peng, P. Y. Ayala, W. Chen, M. W. Wong, J. L. Andres, E. S. Replogle, R. Gomperts, R. L. Martin, D. J. Fox, J. S. Binkley, D. J. Defrees, J. Baker, J. J. P. Stewart, M. Head-Gordon, C. Gonzalez, and J. A. Pople, *Gaussian*-94, Gaussian, Inc., Pittsburgh, PA, 1995.
12. H. B. Schlegel, *J. Comput. Chem.*, **3,** 211 (1982).
13. W. J. Hehre, L. Radom, J. A. Pople, and P. v. R. Schleyer, *Ab Initio Molecular Orbital Theory*, John Wiley & Sons, New York, 1986.
14. D. A. McQuarrie, *Statistical Mechanics*, Harper & Row, New York, 1976.
15. R. G. Parr and W. Yang, *Density Functional Theory of Atoms and Molecules*, Oxford University Press, New York, 1989.
16. (a) A. D. Becke, *J. Chem. Phys.*, **98,** 5648 (1993); (b) A. D. Becke, *Phys. Rev. B*, **38,** 3098 (1988).
17. C. Lee, W. Yang, and R. G. Parr, *Phys. Rev. B*, **37,** 785 (1988).
18. K. Fukui, *Acc. Chem. Res.*, **14,** 363 (1981).
19. C. González and H. B. Schlegel, *J. Phys. Chem.*, **94,** 5523 (1990).
20. R. F. W. Bader, *Atoms in Molecules. A Quantum Theory*, Clarendon Press, Oxford, 1990.
21. F. W. Biegler-König, R. F. W. Bader, and T. H. Wang, *J. Comput. Chem.*, **3,** 317 (1982).

22. P. L. A. Popelier, *Comp. Phys. Commun.*, **93,** 212 (1996).
23. (a) A. E. Reed, R. B. Weinstock, and F. Weinhold, *J. Chem. Phys.*, **83,** 735 (1985); (b) A. E. Reed, L. A. Curtiss, and F. Weinhold, *Chem. Rev.*, **88,** 899 (1988).
24. D. Cremer and E. Kraka, *J. Am. Chem. Soc.*, **107,** 3800 (1985).
25. MP2/6-31G*, B3LYP/6-311 + G(3df,2p), and MP2/6-311G + (3df,2p) charge densities were also analyzed. We could not locate a ring critical point using the MP2/6-31G* charge density whereas the other two highest level charge densities produced almost coincident BCP properties and an identical topology compared with the B3LYP/6-31G* and QCISD/6-31G* analyses.
26. (a) Charge densities computed using more flexible basis sets did not render a C3—N7 BCP either at the B3LYP/D95* or B3LYP/6-311G(2d,2p) levels. (b) Further characterization of the C3—N7 interaction may be gained by analyzing the Laplacian of the electron density $\nabla^2\rho(\vec{r})$.[20] Thus, a (3, +1) critical point [local depletion of $\rho(\vec{r})$] on the valence shell of the C3 atom, is found to be aligned with a (3, −1) critical point [secondary local concentration of $\rho(\vec{r})$] on the valence shell of the N7 atom.
27. (a) D. Cremer and E. Kraka, *Angew. Chem. Int. Ed. Engl.*, **23,** 627 (1984); (b) S. Grimme, *J. Am. Chem. Soc.*, **118,** 1529 (1996).
28. Bond orders were computed by means of the following expression (see ref. 20): $n = \exp[A(\rho_c(\vec{r}_c) - B)]$, where the A and B parameters were obtained by a least-square fitting procedure assigning $n = 1$ to methylamine, $n = 2$ to formaldimine, and $n = 3$ for hydrogen cyanide at the MP2/6-31G* and B3LYP/6-31G* levels.
29. (a) ΔH and ΔG *ab initio* values were computed using MP2(FC)/6-31G* frequencies and electronic energies approximated in an additive fashion as follows: E[QCISD(T)/-311 + G(3df,2p)] ≈ E[QCISD(T)/6-31G*] + E[MP2/6-311 + (3df,2p)] − E[MP2/6-31G*]. See L. A. Curtiss, P. C. Redfem, B. J. Smith, and L. Radom, *J. Chem. Phys.*, **104,** 5148 (1996); (b) ΔH and ΔG DFT values were computed using the B3LYP/6-31G* frequencies and B3LYP/6-311 + G(3df,2p)//B3LYP/6-31G* electronic energies. (c) At the MP2/6-31G* and B3LYP/6-31G* levels, $\Delta H_{\mathrm{vib}}(T)$ and $\Delta S_{\mathrm{vib}}(T)$ were scaled using the recommended frequency scaling factors: A. P. Scott and L. Radom, *J. Phys. Chem.*, **100,** 16502 (1996).
30. Although the results of the IRC calculations presented in Figure 2 could suggest some discontinuity near the TS, we checked that no HOMO-LUMO crossing takes place during the evolution of the system. A CISD/6-31G*//MP2/6-31G* single-point calculation at the TS also confirms that the singlet wave function is absolutely dominated by the HF reference wave function.
31. B3LYP/6-31G* tends to reinforce slightly the interaction between formaldimine and cyanoketene as compared with the MP2/6-31G* level. A nonplanar *cis*-zwitterionic intermediate[8] was located on the B3LYP/6-31G* PES. This intermediate is characterized by a C(ketene)—N(imine) bond distance of 1.608 Å and a notable charge transfer of 0.43 e from formaldimine to cyanoketene. However, only 0.6 kcal/mol at the B3LYP/6-31G* level is required to produce fragmentation of this zwitterion passing through the corresponding TS to yield the cyanoketene−formaldimine planar van der Waals cis-complex (0.5 kcal/mol more stable than the zwitterion). The inclusion of ZPVE provokes the disappearance of the zwitterionic intermediate on the PES given that the TS for fragmentation turns out to be 0.1 kcal/mol more stable than the zwitterion.